

# A GRID CONNECTED VARIABLE SPEED WIND ENERGY CONVERSION SYSTEM

Mônica M. Reis, Rafael M. G. Nascimento, Bruno L. Soares,

Samara A. M. Fava, Elidivane M. de Freitas, Carlos E. A. Silva, and Demercil S. Oliveira Jr.

Federal University of Ceará - UFC, Department of Electrical Engineering, Group of Power Processing and Control – GPEC,

Fortaleza – CE – Brazil

[demercil@dee.ufc.br](mailto:demercil@dee.ufc.br), [mon-m-r@uol.com.br](mailto:mon-m-r@uol.com.br)

**Abstract** - The wind energy system presented in this paper uses a permanent magnet generator connected to a three-phase semi-controlled rectifier. Although an acceptable THD and power factor result, the proposed converter is simple, cheaper, and robust. Additionally, a single-phase PWM inverter is also employed in the grid connection. The inverter uses a double hysteresis in the control of the current injected in the grid, what implies reduced switching losses. Analysis and experimental results are presented for a 5 kW prototype.

**Keywords** – Conversion system, permanent magnet generator, wind energy system.

## I. INTRODUCTION

In recent years, many wind energy conversion techniques have been used for interconnection to the grid. Power electronic converters allow using various topologies with increase of power extraction. In [1] a variable speed wind energy conversion system (VSWECS) connected to the grid is presented. This system consists in a permanent magnet generator PMG connected to a power electronic system, which is composed of a PWM rectifier associated to a PWM inverter, as the output power is applied in the grid. The power factor correction is based on the principle to shape the line current as the line voltage. The control circuit used in the inverter uses a PLL in order to obtain the reference current and an input voltage loop in order to keep the input voltage constant. The maximum power point tracker (MPPT) is obtained by the measurement of the rotor speed of the wind turbine, and adjusting the power reference.

The topology proposed in [2] is similar to that in [1], although the MPPT implemented consists in the measurement of the power and the previous acknowledgment of the machine and turbine parameters. In order to control the current injected to the grid, a hysteresis controller was used.

The VSWECS proposed in [3] consists in a PMG connected to the grid through a back-to-back converter composed by only four IGBT's, what reduces cost. The PMSG output is first converted to dc voltage, inverted and then connected the grid. The rectifier reference current is generated by a PLL and the MPPT is based on the principle of perturbation and observation. The inverter control is performed by using PLL (Phased Locked Loop), and keeping the dc link voltage constant.

These systems are expensive and complex due to the number of IGBT's and the gate drive circuits. Also, the possibility of short-circuit in a leg reduces robustness.

The wind system proposed in [4] consists of a PMSG connected to a three-phase diode rectifier associated to a dc-dc boost chopper and with the output connected to a PWM inverter. The reference current of the boost converter is obtained from the predetermined maximum output torque pattern, according to the generator speed. The active power is controlled by q-axis current whereas the reactive power can be controlled by d-axis current. The phase angle of utility voltage is detected using PLL software in d-q synchronous reference frame. The system configuration of the conversion system in [5] is constituted by a six-phase permanent magnet synchronous generator, six-phase diode rectifier circuit, multiple boost converter, breaking chopper, and dual three-phase PWM inverter, as the implemented MPPT is similar to that in [3]. Such systems have great number of switching and diodes increasing the circuit losses. The system employs breaking chopper to step up the voltage and reduce the losses in the circuit. Although robustness and cost are more attractive aspects than those in the previous topologies, the presence of an additional series converter compromises efficiency and introduces higher harmonic distortion in the generator.

Then, this paper proposes a topology feasible for PMSG that improves robustness and efficiency introducing acceptable harmonic content in the generator currents.

## II. WIND ENERGY CONVERSION SYSTEM

The wind energy conversion system in Fig. 1 is composed of a PMSG rated at 5 kVA connected to a semi-controlled rectifier, composed of three IGBT's and three diodes. The rectifier is responsible for the MPPT and power factor correction.

The MPPT uses the principle of perturbation and observation. The dc-link voltage  $V_{dc}$  is considered constant. The average current  $I_{dc}$  is measured and according to the difference between the current sampling  $I_{dc}(n)$  and the previous value  $I_{dc}(n-1)$ , the reference current amplitude is changed.

Power factor correction is performed using hysteresis control [6], which consists in establishing maximum and/or minimum current limits, and the switching instants occur when the current limits are reached.

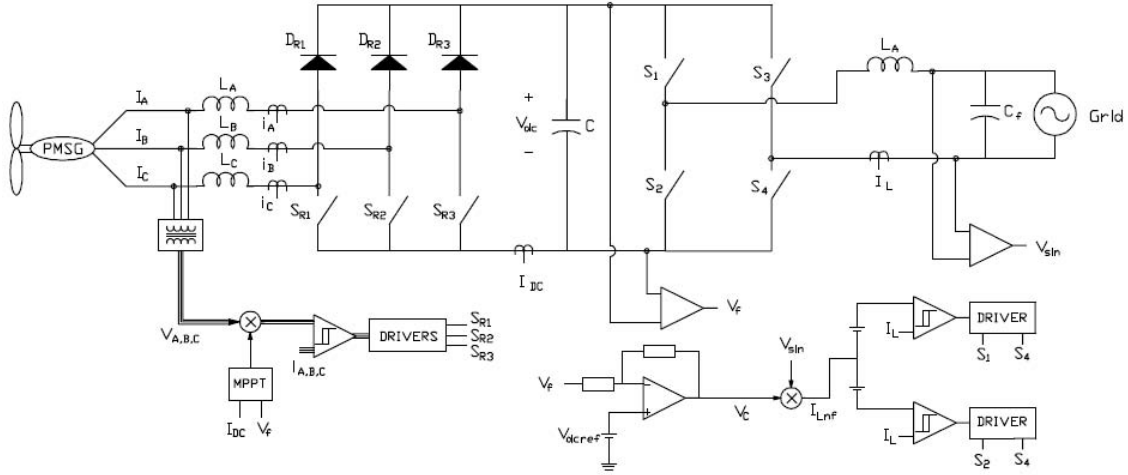


Fig. 1. – Schematic diagram of the wind system proposed.

The dc-ac stage of the wind system is a single-phasefull-bridge topology that employs two IGBT's operating at low frequency and two IGBT's operating at high frequency, what increases efficiency and provides reduced harmonic content of the current injected to the grid. The inverter is controlled by double hysteresis control and the rms current injected to the grid provides regulation of the dc-link voltage.

#### A. Wind Turbine Performance

Let us consider that an amount of wind mass  $m$  and density  $\rho_a$  flowing with speed  $u$  in the axial direction of the wind turbine has some kinetic energy. The available wind power  $P_v$  is the derivative of the kinetic energy with regard to time, given by (1):

$$P_v = \frac{1}{2} \cdot \rho_a \cdot A_v \cdot u^3 \quad (1)$$

The extracted mechanical power  $P_m$  from the available wind power  $P_v$  is determined by the power coefficient  $C_p$ , according to (2).

$$P_m = C_p \cdot P_v = C_p \cdot \left( \frac{1}{2} \cdot \rho_a \cdot A_v \cdot u^3 \right) \quad (2)$$

The performance of the power coefficient in wind turbines is determined by manufacturers through tests carried out in wind tunnels. The value of  $C_p$  is a function of the wind speed  $u$ , rotation speed of the turbine  $\omega_g$ , pitch angle  $\beta$ , and the aerodynamic characteristics of the turbine.

The power coefficient curve for a given wind turbine is presented in equation (3):

$$C_p = C_1 \cdot \left( \frac{C_2}{\lambda_i} - C_3 \cdot \beta - C_4 \right) \cdot e^{\frac{C_5}{\lambda_i}} + C_6 \cdot \lambda \quad (3)$$

where  $\lambda_i$  is a parameter given in (4).

$$\frac{1}{\lambda_i} = \frac{1}{\lambda + 0.08 \cdot \beta} - \frac{0.035}{\beta^3 + 1} \quad (4)$$

In the simulation tests, the following values for the constants mentioned in (3) are considered:

$C_1 = 0.5176$ ,  $C_2 = 116$ ,  $C_3 = 0.40$ ,  $C_4 = 5$ ,  $C_5 = 21$ ,  $C_6 = 0.0068$

These values are given for a three-bladed wind turbine, with similar aerodynamic characteristics to that used in the system. The value of  $\beta$  chosen for simulation is  $0^\circ$ , as maximum  $C_p$  is obtained in this condition.

#### B. Generator Characteristics

The electrical machine used in the system is a permanent magnet synchronous generator (PMSG) rated at 5kW, 1000rpm, 7 pole pairs, and axial flux. The dynamic model of the machine is obtained in [8], described by expressions (5) to (8).

$$T_e = \frac{E_a \cdot I_a + E_b \cdot I_b + E_c \cdot I_c}{\omega_g} \quad (5)$$

$$J \cdot p \cdot \varpi_g = T_m - T_e - B \cdot \varpi_g \quad (6)$$

$$p \cdot \theta_g = \omega_g \quad (7)$$

$$p \cdot \theta_r = P \cdot \omega_g \quad (8)$$

where :

- $T_e$  Electrical torque;
- $T_m$  Mechanical torque;
- $I_a, I_b, I_c$  Generator line currents;
- $E_a, E_b, E_c$  Neutral-to-phase induced electromotive forces;
- $p$  Differential operator;
- $\theta_r$  Angle that defines the mechanical position of the rotor;
- $\theta_g$  Angle that defines the electrical position of the rotor

The physical parameters of the machine such as phase resistance, self-inductance, and mutual inductance are determined from several evaluation tests described in [7], as a similar PMG rated at 1 kW was used for battery charging.

#### C. Rectifier

The rectifier operates as a boost converter. When the switches ( $S_{r1}$ ,  $S_{r2}$ ,  $S_{r3}$ ) are turned on the current flows through them, and the currents through the inductors will increase, while the diodes ( $D_1$ ,  $D_2$ ,  $D_3$ ) are reverse biased and capacitor  $C$  supplies power to the load. When the switches are turned

off, the diodes ( $D_1, D_2, D_3$ ) are forward biased, and the current will flow through them. The energy stored in the inductor will be transferred to the load.

The equivalent circuit is shown in Fig. 2, as  $V_{S1}, V_{S2}$ , and  $V_{S3}$  are the instantaneous voltages seen by the circuit, which is controlled by the switches.

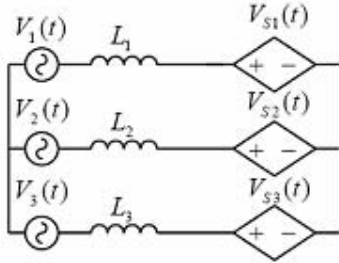


Fig. 2. Rectifier equivalent circuit seen from the input.

Then the following equations are obtained as [7]:

$$V_{L1}(t) = V_1(t) + \frac{-2V_{S1}(t) + V_{S2}(t) + V_{S3}(t)}{3}$$

$$V_{L2}(t) = V_2(t) + \frac{V_{S1}(t) - 2V_{S2}(t) + V_{S3}(t)}{3} \quad (9)$$

$$V_{L3}(t) = V_3(t) + \frac{V_{S1}(t) + V_{S2}(t) - 2V_{S3}(t)}{3}$$

$$I_1(t) = \frac{3V_1(t) - 2V_{S1}(t) + V_{S2}(t) + V_{S3}(t)}{3L_s}$$

$$I_2(t) = \frac{3V_2(t) + V_{S1}(t) - 2V_{S2}(t) + V_{S3}(t)}{3L_s} \quad (10)$$

$$I_3(t) = \frac{3V_3(t) + V_{S1}(t) + V_{S2}(t) - 2V_{S3}(t)}{3L_s}$$

Power factor control and maximum power point tracking (MPPT) are performed by the rectifier. The employed MPPT algorithm consists in measuring the dc-link current  $I_{dc}$ , considering that voltage  $V_{dc}$  is maintained constant. Then the operating point is perturbed by increasing or decreasing the reference current amplitude. If the new value of the current is greater than the previous one, the reference current amplitude is further increased. Otherwise, the reference current must be decreased.

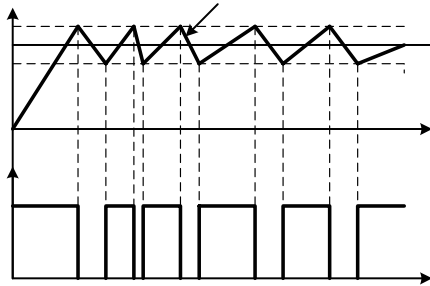


Fig. 3. Current waveform and instantaneous output voltage using hysteresis control.

The MPPT operates associated to power factor control, which uses the principle of hysteresis control [9]. The input current in each phase,  $I_A, I_B$ , and  $I_C$  are measured and compared to the respective current reference  $I_{REF(A)}, I_{REF(B)}$ , and  $I_{REF(C)}$  and switching occurs when the current limits are

reached, as shown Fig. 3, although variable switching frequency results.

#### D. Inverter

The dc-ac stage is a current-controlled full-bridge single-phase inverter. This inverter was chosen because for a three-phase inverter the dc link voltage required must be greater than 700 V (the available grid voltage is equal to 220/380V) and because it is recommended for high power applications.

The control is obtained using double hysteresis and three-level modulation [10]. Current-controlled inverters are used in applications where it is desired to control the output current. The control system operates in closed loop with output current feedback.

The hysteresis comparator operates as follows. The output current, which is given by a current transducer, is compared with the reference signal waveform. The double hysteresis current-controlled inverter uses two reference signals. Thus, it generates a three-level control to drive the switches, what reduces significantly the harmonic distortion of the output current.

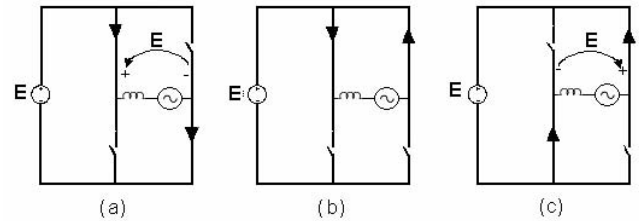


Fig. 4. Stages of three-level modulation: (a) First stage:  $+E$ ; (b) Second stage: 0; (c) Third stage:  $-E$ .

### III. SIMULATION RESULTS

The three-phase three-switch PWM Boost rectifier was analyzed by simulation, as the parameters given in Table I are employed.

Fig. 5 shows the line voltage and the inductor current, which are in phase. The voltage waveform is sinusoidal along all the period, but the current waveform is sinusoidal only during the positive half-cycle. In the negative half-cycle the currents have an irregular waveform as THD is about 18%. Although the current waveform is irregular, the result is considered more satisfactory than in the previous PMG application [7].

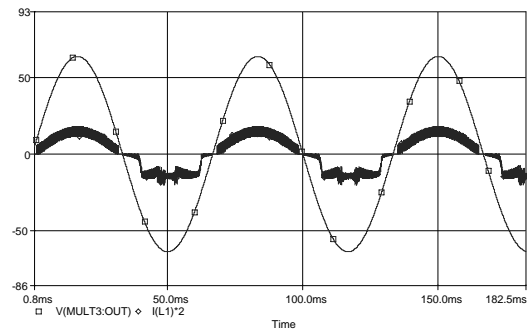


Fig. 5. Simulation results: line voltage and inductor current.

**TABLE I**  
**Rectifier specifications and parameters.**

Rms input voltage amplitude range	100V – 220V
Frequency range of the input voltage	20 – 70 Hz
Output voltage range	330 - 400 V
Switching frequency range	$f_s=20 - 35 \text{ kHz}$
Input inductors	700 $\mu\text{H}$
Input power	0 - 5.5kVA

The proposed inverter was simulated in PSPICE, as the parameters set in Table II is used.

**TABLE II**  
**Inverter specifications and parameters.**

Dc link voltage	330V - 400 V
Grid voltage	$V_{out}=220 \text{ V}$
Grid frequency	$f_{grid}=60 \text{ Hz}$
Output inductor	$L_I=5 \text{ mH}$
Switching frequency	$f_s=20 - 35 \text{ kHz}$
Output power	0 - 5kVA

Fig. 6 shows the load current following the double hysteresis reference.

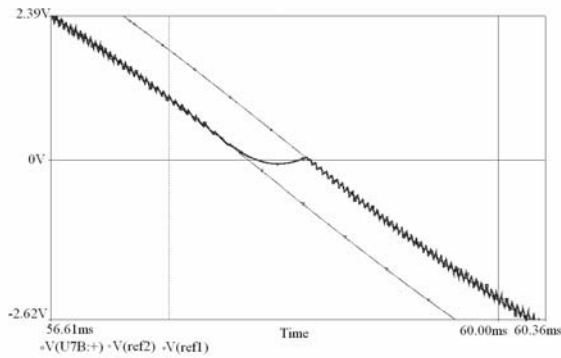


Fig. 6. Current controller response.

Fig. 7 shows the sinusoidal waveform obtained from the simulation of the 110-VAC 60-Hz full-bridge inverter.

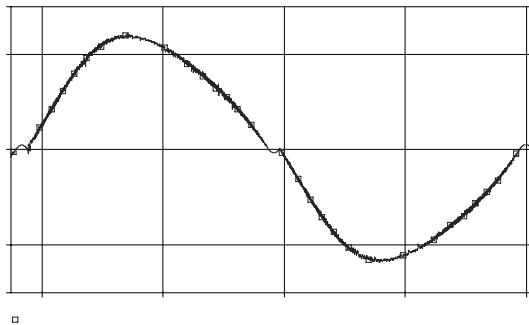


Fig 7. Nearly sinusoidal load current waveform.

The output voltage follows the reference current and was adjusted for a peak output current  $I_L=12\text{A}$  and a frequency of 60Hz.

The total harmonic distortion of the load current is about 6.9%.

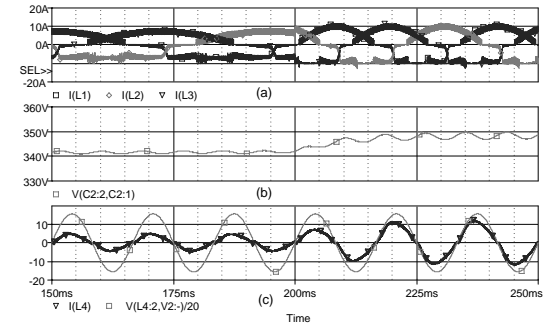


Fig. 8. (a) Currents through phases A, B, and C (b) Dc-link voltage, (c) Grid voltage and current waveforms.

The feedforward control operation is show in fig. 8, where a load step is introduced at 200ms. It consists in adjusting the grid current to maintain the dc-link voltage constant.

#### IV. EXPERIMENTAL RESULTS

In Fig. 9 the current waveforms for an input voltage equal to 220 V are presented , and Fig. 10 shows one of them and the respective voltage. The obtained power factor was 0.957, which is considered satisfactory.

This value is less than the expected result, due to the harmonic content of the current, which is about 16.24%, as seen in Fig. 13.

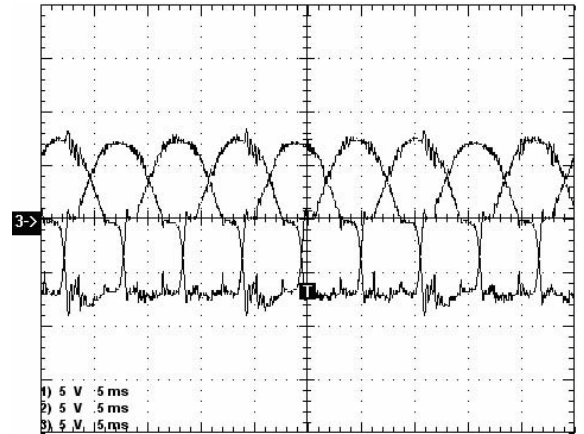


Fig. 9. Rectifier current waveform for input voltage of 220 V (5 A/div, 5 ms/div).

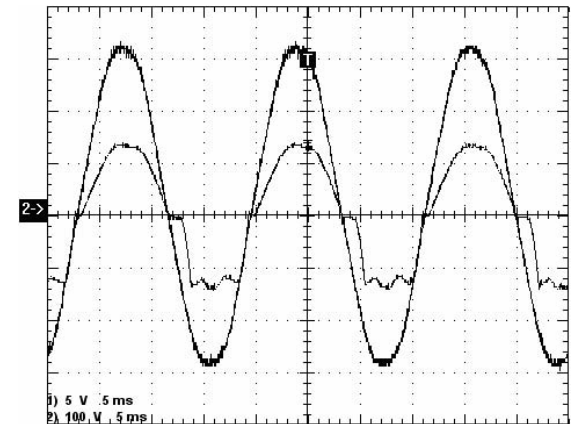


Fig. 10. Rectifier current (5 A/div) and voltage waveform of phase A (100 V/div).

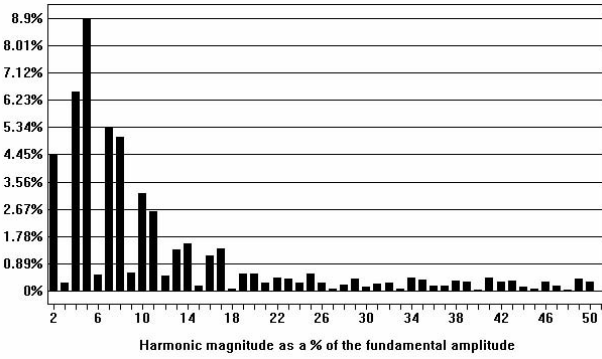


Fig. 11. Harmonic content of the input current waveform shown in Fig. 10.

The proposed inverter prototype was implemented and tested. The results obtained presented in Fig. 12 show the inductor current and the grid voltage. Fig 13 shows the grid voltage and current injected by the inverter.

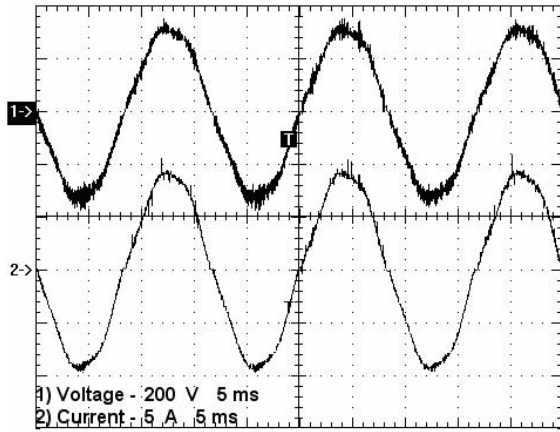


Fig. 12. Inductor voltage (200 V/div, 5 ms/div) and current waveforms (5 A/div, 5 ms/div) for a voltage input equal to 350 V.

For the specified parameters, the rms output current of the inverter is 6.51A and a power factor is 0.995. The total harmonic distortion in the current waveform is about 4.81%. The third and the fifth harmonics are the most relevant components. Fig. 14 shows the aforementioned harmonic contents.

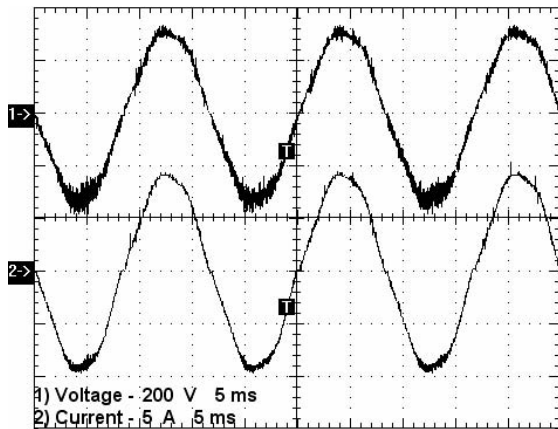


Fig. 13. Grid voltage (200 V/div, 5 ms/div) and current waveforms (5 A/ div, 5 ms/div) for an input voltage equal to 350V.

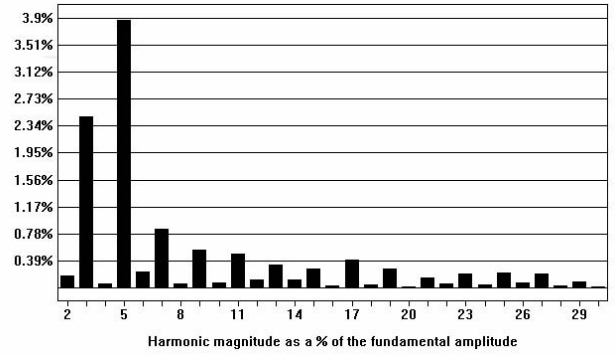


Fig. 14. Harmonic content of the current waveform shown in Fig. 11.

Table III shows the results obtained for input voltage of 350 V.

**TABLE III**  
**Experimental results regarding the proposed system**

Input voltage	$V_A=V_B=V_C=200\text{ V}$
Input current	$I_A=I_B=I_C=5,1\text{ A}$
Dc-link voltage	$V_{dc}=338,5\text{ V}$
Output voltage	$V_{grid}=227\text{ V}$
Output current	$I_L=7,17\text{ A}$
Current A THD	16.24%
Gird Current THD	4.81%
Output Power factor	$F_p=0.995$
Output Power	$P_o=1632\text{ W}$

The complete system was tested and the dc link voltage was maintained regulated by the inverter input voltage control loop. Fig. 14 shows the dynamic response for a step in the current reference of the generator line currents. The response is slow in order to keep low THD of the injected current grid and achieve satisfactory voltage regulation. Fig. 15 shows the measured efficiencies and validates the expected improvement when compared with similar works.

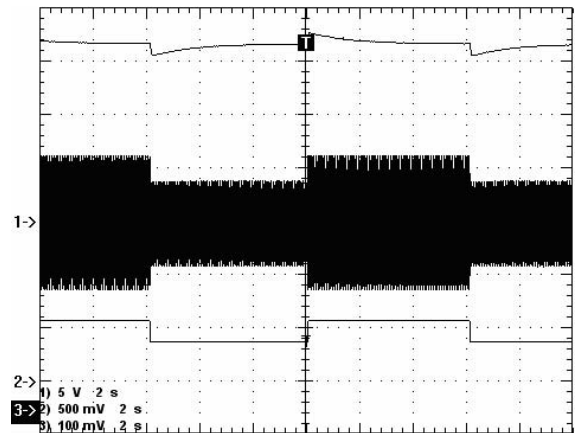


Fig. 14. Dc-link voltage, grid current waveform and input current reference.

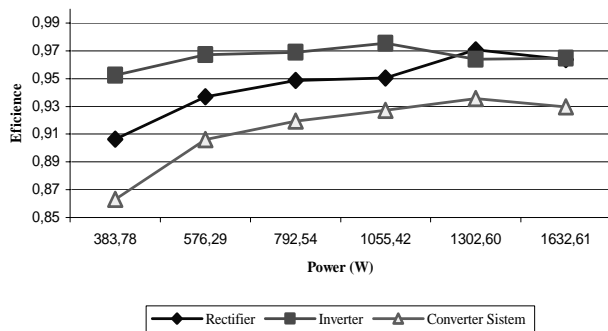


Fig. 15. Efficiency versus output power when the input and the output voltage are 220 V.

## V. CONCLUSION

This paper has presented a wind generation system with low harmonic content in the generator currents and optimal extraction of power. The whole system was simulated and implemented experimentally. MPPT allows the extraction of maximum power, by only measuring dc-link voltage and current. This is achieved without the knowledge of wind turbine parameters.

The experimental results and the voltage controller response can be considered satisfactory. The presented system has some advantages such as simplicity, high efficiency, low cost and robustness. The double hysteresis control causes THD reduction and increases efficiency.

## ACKNOWLEDGEMENT

The authors would like to thank FUNCAP for the financial support and incentive to scientific research, ENERSUD for the donation of a wind generator, FINEP and ELETROBRAS for the financial incentive, and the people who contributed with the development of this work.

## REFERENCES

- [1] A.B. Raju, B.G. Fernandes, K. Chatterjee, "A UPF power conditioner with maximum power point tracker for grid connected variable speed wind energy conversion system", IEE Power Electronics Systems and Applications, 2004. pp. 107-112, November 2004.
- [2] I. Schiemenz, M. Stiebler, "Control of a permanent magnet synchronous generator used in a variable speed wind energy system", Electric Machines and Drives Conference, 2001. IEEE International 2001 pp. 872 – 877.
- [3] A.B. Raju, B.G. Fernandes, K. Chatterjee, "A simple maximum power point tracker for grid connected variable speed wind energy conversion system with reduced switch count power converters", Power Electronics Specialist Conference, 2003. PESC 03. IEEE 34th Annual, Vol. 2, pp. 748-753, June 2003.
- [4] Seung-Ho Song; Shin-il Kang; Nyeon-kun Hahm; "Implementation and control of grid connected AC-DC-AC power converter for variable speed wind energy conversion system", Applied Power Electronics Conference and Exposition, 2003. APEC '03. Eighteenth Annual IEEE, Vol 1, pp. 154-158, February. 2003.
- [5] X. Xin, L. Hui, "Research on multiple boost converter based on MW-level wind energy conversion system", Electrical Machines and Systems, 2005. ICEMS 2005. Proceedings of the Eighth International Conference on, Vol. 2, pp. 1056-1049, September 2005.
- [6] M. T. Galelli, "Controle por histerese com frequência quase constante de um pré-regulador boost". 2005. Dissertation (Electrical Engineer Mastership), Universidade Federal de Uberlândia.
- [7] D. S Oliveira Jr, L. H. S. C. Barreto, I. R. Machado , T. A. Bernardes, "Avaliação do Aproveitamento da Energia Elétrica Gerada por um Sistema Eólico para Carregamento de baterias, Simpósio Brasileiro de Sistemas Elétricos, 2006.
- [8] A. F. Souza, "Retificadores Monofásicos de Alto Fator de Potência com Reduzidas Perdas de Condução e Comutação Suave". 1998. 181f. Thesis (Electrical Engineer Doctorate) – Pos-Graduation Program in Electrical Engineer, Universidade Federal de Santa Catarina, Florianópolis.
- [9] C. H. Treviso, V. J. Farias, J. B. Vieira Jr. and L. C. de Freitas, "A three phase pwm boost rectifier with high power factor operation and an acceptable current THD using only three switches", Ropesc.
- [10] I. Barbi, D.C. Martins, "Introdução ao Estudo dos Conversores CC-CA", Author Edition, Florianópolis, 2005.